J Vet Sci. 2021 Jan;22(1):e3
https://doi.org/10.4142/jvs.2021.22.e3
pISSN 1229-845X·eISSN 1976-555X

Journal of Veterinary Science

Original Article
Medical Imaging

Check for updates

Age-related change in shear elastic modulus of the thoracolumbar multifidus muscle in healthy Beagle dogs using ultrasound shear wave elastography

Akari Tokunaga, **Miki Shimizu** *

Department of Veterinary Diagnostic Imaging, Faculty of Agriculture, Tokyo University of Agriculture and Technology, Tokyo 183-8509, Japan

OPEN ACCESS

Received: Aug 4, 2020
Revised: Oct 19, 2020
Accepted: Oct 30, 2020

***Corresponding author:**
Miki Shimizu
Department of Veterinary Diagnostic Imaging, Faculty of Agriculture, Tokyo University of Agriculture and Technology, 3-5-8 Saiwai-cho, Fuchu, Tokyo 183-8509, Japan.
E-mail: mikivet@me.com

ORCID iDs
Akari Tokunaga
https://orcid.org/0000-0002-4479-8419
Miki Shimizu
https://orcid.org/0000-0002-9172-1131

Conflict of Interest
The authors declare no conflict of interest.

Author Contributions
Conceptualization: Tokunaga A, Shimizu M; Data curation: Tokunaga A; Formal analysis: Tokunaga A; Funding acquisition: Shimizu M; Investigation: Tokunaga A, Shimizu M; Methodology: Tokunaga A, Shimizu M; Project administration: Shimizu M; Resources:

ABSTRACT

Background: Multifidus muscle stiffness decreases in patients with lumbar intervertebral disk herniation; however, age-related changes in humans have not been reported.
Objectives: The reliability of ultrasound shear wave elastography in dogs, and changes in the shear elastic modulus of the thoracolumbar multifidus muscle with aging in dogs, were investigated.
Methods: Twelve beagle dogs were divided into 2 groups based on the age of onset of intervertebral disk herniation: young (aged not exceeding 2 years; 1.3 ± 0.6 years old, n = 5) and adult (4.9 ± 1.2 years old, n = 7). The shear elastic modulus of the multifidus muscle, from the thirteenth thoracic spine to the fourth lumbar spine, was measured using ultrasound shear wave elastography. The length, cross-sectional area and muscle to fat ratio of the multifidus muscle, and the grade of intervertebral disk degeneration, were assessed using radiographic and magnetic resonance imaging examinations.
Results: The length and cross-sectional area of the multifidus muscle increased caudally. In the young group, the shear elastic modulus of the multifidus muscle of the thirteenth thoracic spine was less than that of the third lumbar spine. In the adult group, the shear elastic modulus of the multifidus muscle of first and third lumbar spine was lower than that of the same site in the young group.
Conclusions: Ultrasound can be used to measure shear wave elastography of the thoracolumbar multifidus in dogs. If the multifidus muscle stiffness decreases, we should consider age-related change.

Keywords: Aging; elasticity; elastic modulus; intervertebral disk degeneration; vertebra

INTRODUCTION

Ultrasound shear wave elastography (SWE) is a reproducible and non-invasive method for measuring tissue elasticity [1]. An ultrasound system with SWE software installed and a high-frequency linear array transducer are required to perform measurements. The transducer is placed on the skin above the target tissue and the region of interest (ROI) in the tissue is set.

Shimizu M; Software: Tokunaga A, Shimizu M; Supervision: Shimizu M; Validation: Shimizu M; Visualization: Tokunaga A, Shimizu M; Writing - original draft: Tokunaga A; Writing - review & editing: Shimizu M, Tokunaga A.

The shot button is pressed to send shear waves to the tissue, and the average of the elastic modulus (kPa) is calculated by the shear wave velocity (m/s).

The multifidus muscle is a segmental muscle, originating from the mamillary process in the lumber spines or the transverse process in the thoracic spines of caudal vertebra, while the insertion is located on the spinous processes of the cranial vertebra [2]. The multifidus muscles help fix the vertebral column and stabilize the trunk during gait [2,3]. Intervertebral disks also help stabilize the spine [4,5], and degenerative changes in them can induce decreased spine stability and change the spine's motion [6].

The multifidus muscle is unisegmentally innervated by the medial branches of the dorsal branches of the lumbar and thoracic spinal nerve [7]. This characteristic innervation of the multifidus muscle allows spinal segmental dysfunction to be detected using electromyography [8]. In humans, muscle atrophy and fat infiltration can be observed in denervated muscle [9], and in those patients with lower back pain, intervertebral disk herniation (IVDH) [10,11] or intervertebral disc degeneration (IVDD) [12] may occur. In veterinary medicine, fat infiltration was observed in the multifidus muscle at lesion site in Dachshunds with IVDH, compared with that observed in dogs with fibrous cartilage embolism [13]. Muscle atrophy of the multifidus muscle was reported in dogs with degenerative lumbosacral stenosis [14]. Changes in muscle structure lead to changes in muscle stiffness [15] and loss of muscle function [16]. Such changes in muscle structure have been evaluated using magnetic resonance imaging (MRI) in both humans and dogs, but muscle stiffness cannot be assessed by MRI.

Measuring muscle stiffness using SWE is a new method for assessing muscle function and degeneration. Some reports in humans have suggested that multifidus muscle stiffness decreased in patients with unilateral lumbar IVDH [17] and increased in patients with lower back pain [18,19]. Therefore, measuring muscle stiffness of the multifidus may help to evaluate spine stability and pathology, as well as investigate the prognostic and therapeutic effects of any approaches instituted.

Aging can also cause muscle changes, such as loss of mass and fat infiltration in human skeletal muscle [20-23]. As a result, muscle stiffness changes [15,24]. However, age-related changes of the shear elastic modulus in the lumbar multifidus muscle in healthy people have not been reported [25]. There have been no reports about the utility of ultrasound shear wave elastography for the assessment of the multifidus muscle in dogs.

The aim of this study was to assess the reliability of measuring the shear elastic modulus of the thoracolumbar multifidus muscle using ultrasound SWE in dogs. We also wished to assess age-related changes by comparing the shear elastic modulus in dogs based on the age of onset of IVDH, which is a common disc disease, i.e. in young dogs, before the onset of IVDH and in adult dogs, of an age at which IVDH can occur. In addition, we investigated muscle length, muscle cross-sectional area (CSA) and fat infiltration (the muscle to fat ratio) of the multifidus muscles, and the grade of IVDD. We hypothesized that the shear elastic modulus decreases when fat infiltrates the multifidus muscle and that the grade of disc degeneration progresses with age.

MATERIALS AND METHODS

Animals

This research was approved by the Institute of Experimental Animal Science of the Tokyo University of Agriculture and Technology (No. 30-142). Twelve healthy Beagle dogs were divided into 2 groups. The young group (n = 5) comprised 3 females and 2 spayed females, aged 1.3 ± 0.6 years (mean ± standard deviation), weight 9.6 ± 0.8 kg (mean ± standard deviation), and a median body condition score (BCS) of 3 out of 5 (range, 3–4). The adult group (n = 7) comprised 4 castrated males, 2 females and 1 spayed female, aged 4.9 ± 1.2 years, weight 10.6 ± 1.2 kg, and a median BCS of 3 (range, 1–4). The dogs were free from haematological, musculoskeletal and neurological abnormalities, based on physical, haematological, orthopaedic, neurological and radiographic examination.

Study protocol

The multifidus muscle between the thirteenth thoracic and fourth lumbar spine (T13–L4) was assessed for shear elastic modulus, length, CSA and fat infiltration by ultrasound, radiographic and MRI examination. Five sites of intervertebral disks, between the thoracic vertebra 11 and 12 (T11–T12) and the lumbar vertebra 3 and 4 (L3–L4) were assessed for IVDD using MRI.

Radiographic examination was performed without sedation. The ventrodorsal and lateral projections of the thoracic and lumbar spine were acquired and the number of vertebrae, the presence of vertebral malformation and any soft tissue abnormalities were confirmed. The length of the multifidus muscle at 5 sites was measured from the cranial dorsal edge of the mamillary process of the caudal vertebra to the caudal dorsal edge of the spinous process of the cranial vertebra in the lateral view (**Fig. 1**).

MRI was performed under anesthesia. Atropine (50 μg/kg; Atropine sulfate injection; Fuso Pharmaceutical Industries, Ltd., Japan) was administered subcutaneously as a premedication for anesthesia, then Propofol (Propofol 1% intravenous injection; Fresenius Kabi Japan, Japan) was intravenously administered (up to 6 mg/kg) until tracheal intubation was possible. Anesthesia was maintained with isoflurane (Animal isoflurane; MSD Animal Health K.K., Japan) in oxygen for the duration of the imaging procedure. MRI of the thoracolumbar spine was performed with a 0.3 Tesla system using a knee coil (AIRIS-alfa comfort 0.3T; HITACHI Medical, Japan). The dogs were positioned in dorsal recumbency with both hindlimbs caudally extended. Thoracolumbar spine tissue was imaged in the sagittal plane

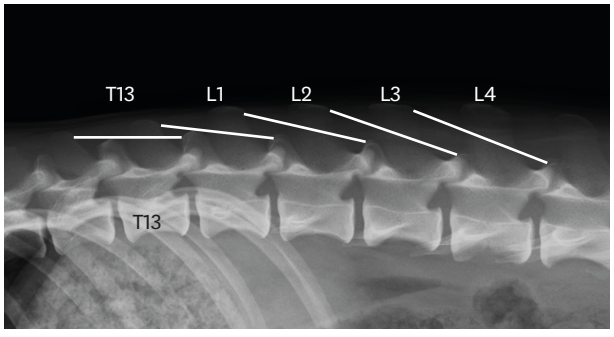

Fig. 1. Measuring muscle length using radiologic images. The length of the multifidus muscle was measured from the cranial dorsal edge of the mamillary process of caudal vertebra to the caudal dorsal edge of the spinous process of cranial vertebra, in lateral view.

https://doi.org/10.4142/jvs.2021.22.e3

with T2-weighted image sequences for position imaging (fast spin-echo sequence: repetition time [TR], 3,000 ms; echo time [TE], 120 ms; slice thickness, 2.5 mm; inter-slice gap, 0.5 mm; flip angle, 90°; field of view, 250 mm; matrix, 288 × 224; acquisition time, 6 min). Then, T1-weighted images were taken (spin-echo sequence: TR, 400 ms; TE, 26 ms; slice thickness, 2.5 mm; inter-slice gap, 0.5 mm; flip angle, 90°; field of view, 250 mm; matrix, 288 × 224; acquisition time, 5 min 58 sec). The transverse images were taken in 3 planes at the level of each intervertebral space centered at the intravertebral disk using the T2-weighted images sequence (fast spin-echo sequence: TR, 4,500 ms; TE, 120 ms; slice thickness, 4.0 mm; inter-slice gap, 0.5 mm; flip angle, 90°; field of view, 150 mm; matrix, 256 × 192 mm; acquisition time, 9 min 36 sec) and the T1-weighted images sequence (spin-echo sequence: TR, 740 ms; TE, 20 ms; slice thickness, 4.0 mm; inter-slice gap, 0.5 mm; flip angle, 90°; field of view, 150 mm; matrix, 256 × 180 mm; acquisition time, 8 min 53 sec). Then, the sagittal and transverse planes of the contrast-enhanced T1-weighted images sequence at the same slice lines. The contrast medium was Gadolinium, with bolus intravenous administration of 0.2 mg/kg meglumine gadopentetate (Magnevist; Bayer, USA). From these MRI images, the configuration and signal intensity of various tissues, such as intraventricular discs, multifidus muscle and spinal cord, were assessed.

The multifidus muscle CSA was measured bilaterally at five sites (n = 10). This was done by manually tracing around the muscle from the transverse image of the T1-weighted images [26] at the level of the center of the intravertebral disk using a DICOM viewer (Osiri X Lite version 11, Pixmeo, Switzerland). The multifidus muscle was defined by the most superficial aspect of the vertebral arch from the spinous process to the articular joint at the medial border. The lateral border was defined by the fascial line of the multifidus muscle from the articular joint to the subcutaneous tissue and the spinous process (**Fig. 2**).

The presumptive fat infiltration of the multifidus muscle was calculated bilaterally at five sites (n = 10) using the signal intensity in the same magnetic resonance image at the CSA using a DICOM viewer. A 5-mm^2 ROI was set at the whitest part in the visceral fat in the same image (**Fig. 2**). The muscle to fat ratio was calculated using the formula [13]:

$$\text{Muscle to fat ratio} = \frac{\text{Muscle mean hyperintensity}}{\text{Subcutaneous fat mean hyperintensity}}$$

Fig. 2. Transverse T1-weighted image at L3-L4 in the adult group. Dotted lines depict where the multifidus muscle and the muscle CSA are calculated. A ROI, 5 mm^2 in area, was set at the whitest part of the visceral fat to calculate the muscle to fat ratio.
CSA, cross-sectional area; ROI, region of interest.

https://doi.org/10.4142/jvs.2021.22.e3

The grade of IVDD at 5 sites was classified from 1 (normal) to 5 (end-state of IVDD), according to the Pfirrmann grading system [27], from the sagittal images of the T2-weighted MR images [28].

Ultrasound shear wave elastography

SWE was performed in sedated dogs. Medetomidine (20 μg/kg; DOMITOR; Nippon Zenyaku Kogyo Co. Ltd., Japan) was intramuscularly administered in the thigh muscle. The dogs were placed in a prone position using a vinyl-covered V-shaped trough with both thoracic limbs extended cranially; both hind limbs were flexed during the examination. The dogs' dorsal region hair was clipped from cranial of the 12th thoracic to caudal of the 4th lumbar of the spinous process in the craniodorsal direction, and from the spinous process to expand beyond the articular process on both left and right sides. The shear elastic modulus of the multifidus muscle was measured using an ultrasound system (Aplio α450, Canon Medical Systems, Japan) with SWE software installed and a 10-MHz linear array transducer (PLT-1005 BT; Canon Medical Systems). The bilateral iliac wing was palpated using the thumb and third finger, and the 6th lumbar spinous process was palpated using the index finger. The spinous processes were sequentially counted cranially until the 12th thoracic, and each spinous process was marked with a pen. Measurement was started at the 13th thoracic multifidus muscle, evenly on the left and right sides. To measure the 13th thoracic multifidus muscle, for example, the 12th and 13th thoracic spinous processes were palpated, and the articular process was identified as being slightly lateral between the 2 spinous processes. The transducer was placed longitudinally between 2 spinous processes and the articular process. If the spinous process and articular process could not be palpated, the processes were confirmed by ultrasound imaging. The articular process was visualized by placing the transducer slightly laterally between the two spinous processes and orienting it approximately 40° outwards. The transducer was placed perpendicular to the skin with no compression force, and gel was generously applied to the skin surface. The multifidus muscle was evaluated longitudinally using a B-mode ultrasound image. The muscle fibres of the multifidus muscle run parallel to the long axis. So, the transducer was directed parallel to the muscle fibres [29]. A 10-mm^2 ROI was set at the belly of the multifidus muscle, avoiding the bones and fascia, and the elastic modulus (kPa) was measured (**Fig. 3**). Ten measurements were recorded at each site.

After the SWE examination, atipamezole (20 μg/kg; ANTISEDAN; Nippon Zenyaku Kogyo Co. Ltd.) was intramuscularly administered to antagonize sedation.

Two sonographers measured the shear elastic modulus of the multifidus muscle. To confirm that the shear elastic modulus of multifidus muscle could be measured in dogs using ultrasound, the researchers performed the same test again, within 1 to 7 days.

Statistical analysis

For the shear elastic modulus of each multifidus muscle, the mean value of 10 measurements was used. The left- and right-side measurements at each site of muscle CSA, muscle to fat ratio and shear elastic modulus were summarized by site. The normality of the data was assessed using the Shapiro-Wilk test. When there was no normal distribution, the data were expressed as medians with interquartile ranges. All data were statistically analyzed using two-way analysis of variance (ANOVA) followed by Bonferroni's multiple comparison test between groups and sites using GraphPad Prism Version 8 (GraphPad Software Inc., USA). Significance was set at $p < 0.05$. The intra- (intraclass correlation coefficients; ICC 1.2) and inter-observer correlation coefficients (ICC 2.2) for the shear elastic modulus of the multifidus muscle were statistically analyzed using IBM SPSS Statistics 20.0 (IBM SPSS Statistics Server; IBM Japan, Ltd., Japan).

Journal of Veterinary Science

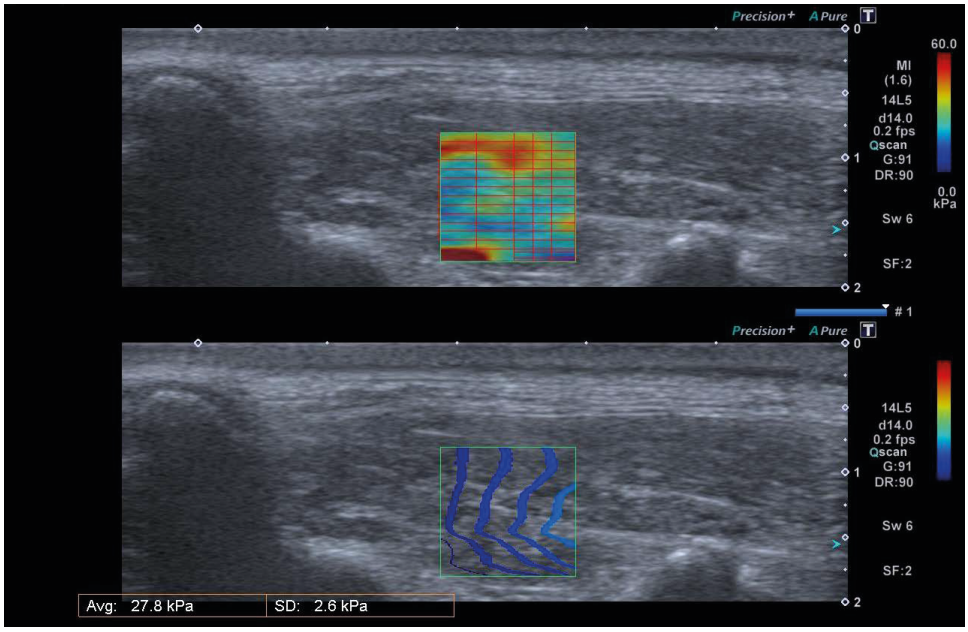

Fig. 3. Ultrasound shear wave elastography on the sagittal image of the 4th lumbar multifidus muscle. A 10-mm^2 ROI was set at the belly of the multifidus muscle. The hardness of the muscle in the ROI is shown in the color-coded area of the upper image, and the propagation of transient shear waves is shown in the bottom image. ROI, region of interest.

RESULTS

The radiographic and MRI examinations showed no abnormal findings in the vertebra, soft tissues around the vertebra or the spinal cord. Muscle length, muscle CSA and muscle to fat ratio results are summarized in **Table 1**. The length and CSA of the multifidus muscle

Table 1. Muscle length, CSA and muscle to fat ratio of the multifidus muscle

Site	Young group (n = 5)	Adult group (n = 7)
Muscle length (cm)		
T13	2.94 (2.89–3.18)	3.12 (3.06–3.25)
L1	3.23 (3.22–3.56)[a]	3.44 (3.34–3.55)
L2	3.36 (3.09–3.66)	3.81 (3.66–3.96)[a,b]
L3	3.57 (3.53–3.95)[a]	3.89 (3.72–4.12)[a,b]
L4	3.67 (3.48–4.14)	4.14 (3.95–4.31)[a,b]
Muscle CSA (mm^2)		
T13	28.8 (27.7–36.5)	38.6 (24.8–45.7)
L1	40.0 (37.3–48.3)[a]	33.5 (27.7–44.4)
L2	64.0 (56.6–83.8)[a,b]	57.4 (46.9–75.8)[a,b]
L3	103.5 (89.7–125.2)[a,b,c]	105.4 (90.0–114.6)[a,b,c]
L4	140.8 (134.8–150.0)[a,b,c,d]	127.2 (107.9–142.9)[a,b,c,d]
Muscle to fat ratio		
T13	0.367 (0.343–0.409)	0.403 (0.323–0.479)
L1	0.378 (0.367–0.431)	0.449 (0.333–0.474)
L2	0.409 (0.379–0.423)	0.387 (0.350–0.470)
L3	0.365 (0.348–0.393)	0.405 (0.304–0.445)
L4	0.364 (0.350–0.402)	0.432 (0.257–0.459)

Data are expressed as medians (interquartile ranges).
CSA, cross-sectional area.
[a]Significant difference from T13 in the same group ($p < 0.05$); [b]Significant difference from L1 in the same group ($p < 0.05$). [c]Significant difference from L2 in the same group ($p < 0.05$). [d]Significant difference from L3 in the same group ($p < 0.05$).

https://doi.org/10.4142/jvs.2021.22.e3

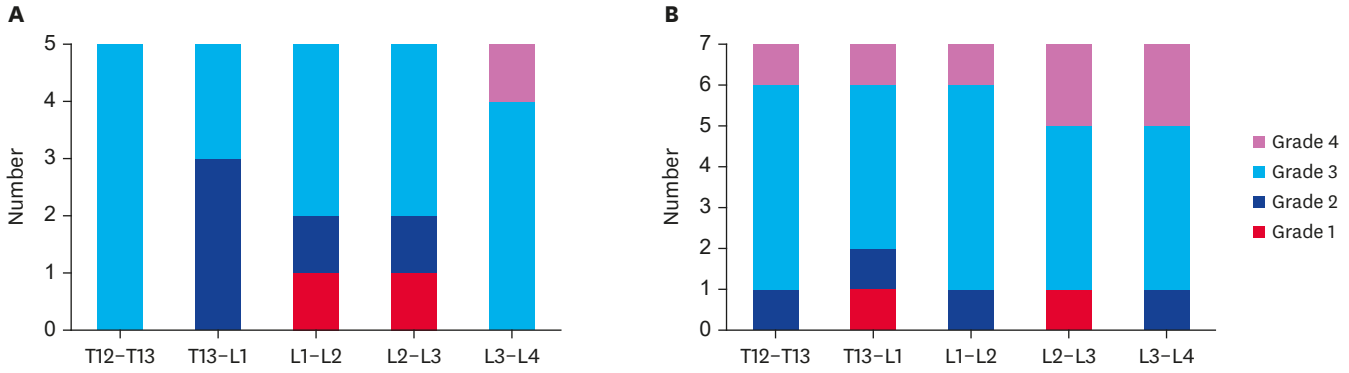

Fig. 4. Stacked bar graph of IVDD grades. (A) In the young group. (B) In the adult group. Data are expressed as medians.
IVDD, intervertebral disk degeneration.

increased more caudally than it did cranially within the same group and in both young and adult groups. There were no significant differences between the 2 groups. There were no significant differences in muscle to fat ratio, within or between groups.

IVDD grades are shown in **Fig. 4**. In the young group, grade 4 IVDD was observed at just one site (4% of the total). In the adult group, grade 4 IVDD was observed at all sites (20% of the total). However, there were no significant differences within or between groups.

SWE examinations

The bilateral iliac wing and 6th lumbar spinous process were palpated in all dogs. In 2 dogs with BCS 4 (one from each of the young and adult groups) it was difficult to palpate the spinous process and articular joint. Obese dogs had more subcutaneous fat, but this did not affect visualization of the multifidus muscle. There were no abnormalities of the multifidus muscle and the transducer could easily be oriented parallel to the muscle fibers. The multifidus muscles at cranial sites were short and small, therefore practice was needed to visualize the muscle fibers, and setting the ROI was limited. In contrast, the longer muscle and increased CSA at caudal multifidus muscle sites made setting the ROI at the muscle belly relatively easy.

The shear elastic modulus results are summarized in **Table 2**. In the young group, the shear elastic modulus of the multifidus muscle at T13 was lower than that at L3 ($p = 0.042$). There were no differences in the shear elastic modulus within the adult group, but it was lower at L1 and L3 compared with the values at the same sites in the young group ($p = 0.048$ and $p = 0.011$, respectively).

The intra- and inter-observer agreement for the shear elastic modulus of the multifidus muscle at all sites was substantial and almost perfect, respectively [30] (**Table 3**).

Table 2. Shear elastic modulus in multifidus muscles (kPa)

Site	Young group (n = 5)	Adult group (n = 7)
T13	21.3 (20.2–22.8)[a]	19.2 (16.0–24.3)
L1	22.0 (20.3–29.7)	16.4 (13.9–19.6)[b]
L2	22.7 (20.5–25.5)	17.6 (14.9–20.5)
L3	26.8 (23.7–29.6)	16.5 (15.8–20.0)[b]
L4	24.9 (20.5–30.2)	19.0 (16.0–21.5)

Data are expressed as medians (interquartile ranges).
[a]Significant difference from L3 in the same group ($p < 0.05$). [b]Significant difference from that of young group at the same site ($p < 0.05$).

https://doi.org/10.4142/jvs.2021.22.e3

Table 3. Inter- and intra-observer agreement for the shear elastic modulus

Site	Intra-observer correlation coefficient, ICC (1.2)	Inter-observer correlation coefficient, ICC (2.2)
Total	0.62	0.82
Left		
T13	0.67	0.52
L1	0.64	0.86
L2	0.94	0.54
L3	0.39	0.72
L4	0.38	0.92
Right		
T13	0.90	0.72
L1	0.73	0.90
L2	0.83	0.91
L3	0.60	0.89
L4	0.44	0.80

ICC, intraclass correlation coefficients.

DISCUSSION

The muscle shear elastic modulus of the lumbar multifidus muscle decreased in adult dogs (aged 4.9 ± 1.2 years) compared with the value seen in young dogs (aged 1.3 ± 0.6 years). This suggests that the shear elastic modulus of the multifidus muscle decreases with age. There were no significant differences in muscle length, muscle CSA, IVDD grade or muscle to fat ratio between the 2 groups. In both groups, the length and CSA of the multifidus muscle were increased at the caudal lumbar region compared with these values at the thoracic region, indicating the multifidus muscles were longer and thicker in this region. These results were similar to a previous report in dogs [31].

IVDH typically occurs around the age of 3 to 6 in chondrodystrophic dog breeds [4], although it has been reported in dogs as young as 2 years [32]. Therefore, in this study the dogs were divided into a young group aged not exceeding 2 years and an adult group aged more than 2 years. Assessment of shear elastic moduli was performed by 2 researchers who were experienced at interpreting SWE. Intra-observer agreement for the shear elastic modulus of the multifidus muscle at each site was almost perfect, except at L3 and L4, where there was fair to moderate agreement. In the thoracic region, the multifidus muscles were short and small, so the setting of the ROI was limited. By contrast, at L3 and L4, the multifidus muscles were longer and larger compared with their size in the thoracic region. The setting of the ROI was easy but could lead to incongruent positioning of the ROI. The interobserver agreement for the shear elastic modulus of the muscle was substantial to almost perfect at each site, except the left side of T13 and L2, which both showed moderate agreement. When taking measurements, the sonographer's wrist was held without an angle. However, when measuring the left side of the muscle at T13 and L2, where the muscles were small and the area for positioning the transducer was limited, differences in wrist angles, estimated at between 15° and 35°, between the sonographers might have occurred and could have influenced interobserver agreement. Further studies into setting the ROI at L3 and L4 and developing methods to obtain reproducible measurements at T13 and L2 are needed.

Muscle stiffness is reduced by muscle oedema, atrophy [33] and fat infiltration [24], and increased when collagen concentration and cross-linking increases [34,35]. Muscle stiffness also increases in patients with Duchenne muscular dystrophy [36]. Stretching exercises can reduce muscle stiffness [37-39].

In the young group, the shear elastic modulus of the multifidus muscles at T13 was lower than that at L3. Although the muscle length and CSA of the multifidus muscle were significantly different between T13 and L3, studies in humans showed no significant correlations between muscle mass and muscle stiffness [33,40,41]. In this study, the elastic shear modulus of the multifidus muscle also showed no change in relation to changes in muscle length or CSA of the multifidus muscle in the adult group. Therefore, any differences in the length and CSA of the multifidus muscle might not be caused by differences in its shear elastic modulus. There are regional functional variations in multifidus muscles along the trunk [3]. During trotting in dogs, the motion of sagittal trunk movement is seen at the mid-trunk of the epaxial muscle [42]. Therefore, the multifidus muscle at T13 may be stretched during trotting. Muscle stiffness decreases with stretching [37-39], so we assumed the stretching effect might be the reason why the shear elastic modulus of the multifidus muscle at T13 was decreased compared with that of L3.

In the adult group, there was no significant difference in the shear elastic modulus of the multifidus muscles among the five measurement sites. However, the shear elastic modulus at L1 and L3 of the multifidus muscle in the adult group was lower compared with that in the young group. Beagle dogs are a chondrodystrophic breed, in which IVDD develops from 2 to 9 months of age [4]. The grade of IVDD increased with the increasing age of the dog [28]. IVDD was observed in both groups. The percentage was similar to previously reported results in chondrodystrophic dogs, most of which had no IVDD-related problems [43]. In the present study, no bulging, protrusion, or extrusion of the disc was observed by MRI in any of the dogs with grade 4 IVDD, and there were no clinical signs. No associations between the grade of IVDD and clinical signs in dogs have been reported [43]. Clinical signs such as back pain would not be observed unless there was compression of the anulus fibrosus, which is capable of nociception [44], or the discs were herniated [45]. The multifidus muscle at L1 and L3 may be influenced by the condition of the T13–L1 and L2–L3 intervertebral disks, respectively [14]. However, there was no difference in IVDD grades between the young and adult groups. Therefore, our hypothesis was rejected and we considered that the shear elastic modulus of the multifidus muscle would not change as a result of IVDD alone. As seen at T13 in the young group, the multifidus muscle at L1 and L3 could be stretched by spinal motion; however, we could not explain why there were segmental differences or why the shear elastic modulus of the multifidus muscle decreased in adult dogs. Further study is needed to confirm the reasons for this.

Sex hormones have been shown to influence the structure of skeletal muscle, predisposition to fat and viscoelastic properties in humans [46-48]. They can also change the shear elastic modulus of muscle. In asymptomatic human adult volunteers aged between 20 and 40 years, the fat fraction in the lumbar multifidus muscle in women was higher than that in men [49]. The shear elastic modulus of the lumbar multifidus muscle in females was lower than that in males [25,50]. There have been few reports showing the relationship between sex hormones and skeletal muscle in dogs [51]. Hence, we did not compare sex differences in this study. Although differences in fat infiltration of muscle due to differences in sex hormones have not been reported, there have been reports that surgically neutered dogs showed an increased risk of obesity [52] and that subcutaneous fat levels were increased in neutered male dogs [53]. Additional studies are therefore necessary to evaluate the relationship between sex hormones and muscle structure and the shear elastic modulus in the multifidus muscle.

Other limitations of the present study include the small number of measurements and the lack of an older age group. The shear elastic modulus can be changed by stretching, so we should investigate performing dynamic evaluation of the shear elastic modulus of multifidus

muscle. Furthermore, the influence of joint function is an important factor in muscle stiffness. We should also consider a method for measuring the shear elastic modulus of the multifidus muscle with better reproducibility. Such future studies should help clarify the mechanism of change in the shear elastic modulus and the segmental difference seen in older dogs. In future, we plan to collect data about SWE in dogs with neurological disease to evaluate multifidus muscle function using SWE.

In conclusion, the present research showed that ultrasound SWE can be used to evaluate the shear elastic modulus of the thoracolumbar multifidus muscle in dogs. The shear elastic modulus of the multifidus muscles was lower in adult dogs compared with the value in young dogs. If the stiffness of the multifidus muscle decreases, we should consider age-related changes.

ACKNOWLEDGEMENT

The authors thank Canon for the free loan of an ultrasound system.

REFERENCES

1. Shimizu M, Ito Y. Change in shear elastic modulus of thigh muscle by changing muscle length using ultrasound shear wave elastography in beagle dogs. Vet Comp Orthop Traumatol. 2019;32(6):454-459.
PUBMED | CROSSREF
2. Evans HE, de Lahunta A, Hermanson JW. The muscular system. In: Evans HE, de Lahunta A, editors. *Miller's Anatomy of the Dog*. 4th ed. St. Louis: Elsevier; 2013, 185-280.
3. Schilling N, Carrier DR. Function of the epaxial muscles in walking, trotting and galloping dogs: implications for the evolution of epaxial muscle function in tetrapods. J Exp Biol. 2010;213(Pt 9):1490-1502.
PUBMED | CROSSREF
4. Kent M. Pelvic limb paresis, paralysis, or ataxia. In Lorenz MD, Coates JR, Kent M, editors. *Handbook of Veterinary Neurology*. 5th ed. St. Louis: Elsevier; 2011, 109-161.
5. Hukins DW, Meakin JR. Relationship between structure and mechanical function of the tissues of the intervertebral joint. Am Zool. 2000;40(1):42-52.
CROSSREF
6. Muriuki MG, Havey RM, Voronov LI, Carandang G, Zindrick MR, Lorenz MA, et al. Effects of motion segment level, Pfirrmann intervertebral disc degeneration grade and gender on lumbar spine kinematics. J Orthop Res. 2016;34(8):1389-1398.
PUBMED | CROSSREF
7. Kitchell RL. Spinal nerves. In Evans HE, de Lahunta A, editors. *Miller's Anatomy of the Dog*. 4th ed. St. Louis: Elsevier; 2013, 611-657.
8. Macintosh JE, Valencia F, Bogduk N, Munro RR. The morphology of the human lumbar multifidus. Clin Biomech (Bristol, Avon). 1986;1(4):196-204.
PUBMED | CROSSREF
9. Dulor JP, Cambon B, Vigneron P, Reyne Y, Nouguès J, Casteilla L, et al. Expression of specific white adipose tissue genes in denervation-induced skeletal muscle fatty degeneration. FEBS Lett. 1998;439(1-2):89-92.
PUBMED | CROSSREF
10. Kader DF, Wardlaw D, Smith FW. Correlation between the MRI changes in the lumbar multifidus muscles and leg pain. Clin Radiol. 2000;55(2):145-149.
PUBMED | CROSSREF
11. Battié MC, Niemelainen R, Gibbons LE, Dhillon S. Is level- and side-specific multifidus asymmetry a marker for lumbar disc pathology? Spine J. 2012;12(10):932-939.
PUBMED | CROSSREF
12. Sun D, Liu P, Cheng J, Ma Z, Liu J, Qin T. Correlation between intervertebral disc degeneration, paraspinal muscle atrophy, and lumbar facet joints degeneration in patients with lumbar disc herniation. BMC Musculoskelet Disord. 2017;18(1):167-173.
PUBMED | CROSSREF

13. Boström AF, Hielm-Björkman AK, Chang YM, Weller R, Davies ES. Comparison of cross sectional area and fat infiltration of the epaxial muscles in dogs with and without spinal cord compression. Res Vet Sci. 2014;97(3):646-651.
PUBMED | CROSSREF

14. Henderson AL, Hecht S, Millis DL. Lumbar paraspinal muscle transverse area and symmetry in dogs with and without degenerative lumbosacral stenosis. J Small Anim Pract. 2015;56(10):618-622.
PUBMED | CROSSREF

15. Niyomchan A, Panichareon B, Siriphorn A, Wongtawatchai T. Age-related structural-mechanical property changes in human peroneus longus muscle. Folia Morphol (Warsz). 2019;78(2):401-407.
PUBMED | CROSSREF

16. D'Antona G, Pellegrino MA, Adami R, Rossi R, Carlizzi CN, Canepari M, et al. The effect of ageing and immobilization on structure and function of human skeletal muscle fibres. J Physiol. 2003;552(Pt 2):499-511.
PUBMED | CROSSREF

17. Alis D, Durmaz ES, Alis C, Erol BC, Okur B, Kizilkilic O, et al. Shear wave elastography of the lumbar multifidus muscle in patients with unilateral lumbar disk herniation. J Ultrasound Med. 2019;38(7):1695-1703.
PUBMED | CROSSREF

18. Chan ST, Fung PK, Ng NY, Ngan TL, Chong MY, Tang CN, et al. Dynamic changes of elasticity, cross-sectional area, and fat infiltration of multifidus at different postures in men with chronic low back pain. Spine J. 2012;12(5):381-388.
PUBMED | CROSSREF

19. Murillo C, Falla D, Rushton A, Sanderson A, Heneghan NR. Shear wave elastography investigation of multifidus stiffness in individuals with low back pain. J Electromyogr Kinesiol. 2019;47:19-24.
PUBMED | CROSSREF

20. Narici MV, Maffulli N. Sarcopenia: characteristics, mechanisms and functional significance. Br Med Bull. 2010;95(1):139-159.
PUBMED | CROSSREF

21. Dahlqvist JR, Vissing CR, Hedermann G, Thomsen C, Vissing J. Fat replacement of paraspinal muscles with aging in healthy adults. Med Sci Sports Exerc. 2017;49(3):595-601.
PUBMED | CROSSREF

22. De Carvalho FG, Justice JN, Freitas EC, Kershaw EE, Sparks LM. Adipose tissue quality in aging: how structural and runctional aspects of adipose tissue impact skeletal muscle quality. Nutrients. 2019;11(11):2553-2566.
PUBMED | CROSSREF

23. Fortin M, Videman T, Gibbons LE, Battié MC. Paraspinal muscle morphology and composition: a 15-yr longitudinal magnetic resonance imaging study. Med Sci Sports Exerc. 2014;46(5):893-901.
PUBMED | CROSSREF

24. Alfuraih AM, Tan AL, O'Connor P, Emery P, Wakefield RJ. The effect of ageing on shear wave elastography muscle stiffness in adults. Aging Clin Exp Res. 2019;31(12):1755-1763.
PUBMED | CROSSREF

25. Koppenhaver SL, Scutella D, Sorrell BA, Yahalom J, Fernández-de-Las-Peñas C, Childs JD, et al. Normative parameters and anthropometric variability of lumbar muscle stiffness using ultrasound shear-wave elastography. Clin Biomech (Bristol, Avon). 2019;62:113-120.
PUBMED | CROSSREF

26. Crawford RJ, Cornwall J, Abbott R, Elliott JM. Manually defining regions of interest when quantifying paravertebral muscles fatty infiltration from axial magnetic resonance imaging: a proposed method for the lumbar spine with anatomical cross-reference. BMC Musculoskelet Disord. 2017;18(1):25-35.
PUBMED | CROSSREF

27. Pfirrmann CW, Metzdorf A, Zanetti M, Hodler J, Boos N. Magnetic resonance classification of lumbar intervertebral disc degeneration. Spine. 2001;26(17):1873-1878.
PUBMED | CROSSREF

28. Bergknut N, Auriemma E, Wijsman S, Voorhout G, Hagman R, Lagerstedt AS, et al. Evaluation of intervertebral disk degeneration in chondrodystrophic and nonchondrodystrophic dogs by use of Pfirrmann grading of images obtained with low-field magnetic resonance imaging. Am J Vet Res. 2011;72(7):893-898.
PUBMED | CROSSREF

29. Alfuraih AM, O'Connor P, Hensor E, Tan AL, Emery P, Wakefield RJ. The effect of unit, depth, and probe load on the reliability of muscle shear wave elastography: variables affecting reliability of SWE. J Clin Ultrasound. 2018;46(2):108-115.
PUBMED | CROSSREF

30. Landis JR, Koch GG. The measurement of observer agreement for categorical data. Biometrics. 1977;33(1):159-174.
PUBMED | CROSSREF

31. Webster EL, Hudson PE, Channon SB. Comparative functional anatomy of the epaxial musculature of dogs (*Canis familiaris*) bred for sprinting vs. fighting. J Anat. 2014;225(3):317-327.
PUBMED | CROSSREF

32. Olby N, Harris T, Burr J, Muñana K, Sharp N, Keene B. Recovery of pelvic limb function in dogs following acute intervertebral disc herniations. J Neurotrauma. 2004;21(1):49-59.
PUBMED | CROSSREF

33. Alfuraih AM, O'Connor P, Tan AL, Hensor EM, Ladas A, Emery P, et al. Muscle shear wave elastography in idiopathic inflammatory myopathies: a case-control study with MRI correlation. Skeletal Radiol. 2019;48(8):1209-1219.
PUBMED | CROSSREF

34. Gosselin LE, Adams C, Cotter TA, McCormick RJ, Thomas DP. Effect of exercise training on passive stiffness in locomotor skeletal muscle: role of extracellular matrix. J Appl Physiol (1985). 1998;85(3):1011-1016.
PUBMED | CROSSREF

35. Wood LK, Kayupov E, Gumucio JP, Mendias CL, Claflin DR, Brooks SV. Intrinsic stiffness of extracellular matrix increases with age in skeletal muscles of mice. J Appl Physiol (1985). 2014;117(4):363-369.
PUBMED | CROSSREF

36. Lacourpaille L, Hug F, Guével A, Péréon Y, Magot A, Hogrel JY, et al. Non-invasive assessment of muscle stiffness in patients with Duchenne muscular dystrophy. Muscle Nerve. 2015;51(2):284-286.
PUBMED | CROSSREF

37. Nakamura M, Ikezoe T, Kobayashi T, Umegaki H, Takeno Y, Nishishita S, et al. Acute effects of static stretching on muscle hardness of the medial gastrocnemius muscle belly in humans: an ultrasonic shear-wave elastography study. Ultrasound Med Biol. 2014;40(9):1991-1997.
PUBMED | CROSSREF

38. Yamauchi T, Hasegawa S, Nakamura M, Nishishita S, Yanase K, Fujita K, et al. Effects of two stretching methods on shoulder range of motion and muscle stiffness in baseball players with posterior shoulder tightness: a randomized controlled trial. J Shoulder Elbow Surg. 2016;25(9):1395-1403.
PUBMED | CROSSREF

39. Miyamoto N, Hirata K, Kanehisa H. Effects of hamstring stretching on passive muscle stiffness vary between hip flexion and knee extension maneuvers. Scand J Med Sci Sports. 2017;27(1):99-106.
PUBMED | CROSSREF

40. Chino K, Ohya T, Kato E, Suzuki Y. Muscle thickness and passive muscle stiffness in elite athletes: implications of the effect of long-term daily training on skeletal muscle. Int J Sports Med. 2018;39(3):218-224.
PUBMED | CROSSREF

41. Nagai T, Schilaty ND, Krause DA, Crowley EM, Hewett TE. Sex differences in ultrasound-based muscle size and mechanical properties of the cervical-flexor and -extensor muscles. J Athl Train. 2020;55(3):282-288.
PUBMED | CROSSREF

42. Ritter DA, Nassar PN, Fife M, Carrier DR. Epaxial muscle function in trotting dogs. J Exp Biol. 2001;204(Pt 17):3053-3064.
PUBMED

43. Bergknut N, Smolders LA, Grinwis GC, Hagman R, Lagerstedt AS, Hazewinkel HA, et al. Intervertebral disc degeneration in the dog. Part 1: anatomy and physiology of the intervertebral disc and characteristics of intervertebral disc degeneration. Vet J. 2013;195(3):282-291.
PUBMED | CROSSREF

44. Willenegger S, Friess AE, Lang J, Stoffel MH. Immunohistochemical demonstration of lumbar intervertebral disc innervation in the dog. Anat Histol Embryol. 2005;34(2):123-128.
PUBMED | CROSSREF

45. Chen C, Cavanaugh JM, Song Z, Takebayashi T, Kallakuri S, Wooley PH. Effects of nucleus pulposus on nerve root neural activity, mechanosensitivity, axonal morphology, and sodium channel expression. Spine. 2004;29(1):17-25.
PUBMED | CROSSREF

46. Bhasin S, Woodhouse L, Casaburi R, Singh AB, Bhasin D, Berman N, et al. Testosterone dose-response relationships in healthy young men. Am J Physiol Endocrinol Metab. 2001;281(6):E1172-E1181.
PUBMED | CROSSREF

47. Sørensen MB, Rosenfalck AM, Højgaard L, Ottesen B. Obesity and sarcopenia after menopause are reversed by sex hormone replacement therapy. Obes Res. 2001;9(10):622-626.
PUBMED | CROSSREF

48. Kubo K, Kanehisa H, Fukunaga T. Gender differences in the viscoelastic properties of tendon structures. Eur J Appl Physiol. 2003;88(6):520-526.
PUBMED | CROSSREF

49. Menezes-Reis R, Bonugli GP, Salmon CE, Mazoroski D, Herrero CF, Nogueira-Barbosa MH. Relationship of spinal alignment with muscular volume and fat infiltration of lumbar trunk muscles. PLoS One. 2018;13(7):e0200198.
PUBMED | CROSSREF

50. Heizelmann A, Tasdemir S, Schmidberger J, Gräter T, Kratzer W, Grüner B. Measurements of the trapezius and erector spinae muscles using virtual touch imaging quantification ultrasound-Elastography: a cross section study. BMC Musculoskelet Disord. 2017;18(1):370-377.
PUBMED | CROSSREF

51. Gunn HM. Differences in the histochemical properties of skeletal muscles of different breeds of horses and dogs. J Anat. 1978;127(Pt 3):615-634.
PUBMED

52. McGreevy PD, Thomson PC, Pride C, Fawcett A, Grassi T, Jones B. Prevalence of obesity in dogs examined by Australian veterinary practices and the risk factors involved. Vet Rec. 2005;156(22):695-702.
PUBMED | CROSSREF

53. Kobayashi T, Koie H, Kusumi A, Kitagawa M, Kanayama K, Otsuji K. Comparative investigation of body composition in male dogs using CT and body fat analysis software. J Vet Med Sci. 2014;76(3):439-446.
PUBMED | CROSSREF